Eur Phys J A (2005) **24,** s1, 49–54
DOI: 10.1140/epjad/s2005-05-008-8

EPJ A direct
electronic only

Nucleon form factors

A review of theoretical models

Dieter Drechsel

Institut für Kernphysik, Universität Mainz, 55099 Mainz, Germany

Received: 27 September 2004 / Published Online: 8 February 2005

Abstract. The general structure of elastic and inelastic nucleon scattering is outlined. The predictions of dispersion relations, chiral perturbation theory, and lattice calculations are reviewed. Special attention is given to the role of the pion cloud at small momentum transfer.

PACS. 13.40.Gp – 11.55.Fv – 13.60.Fz – 13.60.Hb

1 Elastic electron–nucleon scattering

The elastic scattering process $e(k)+N(p) \to e'(k')+N'(p')$ may be described by the Mandelstam variables

$$s = (k+p)^2\,, \quad t = (k'-k)^2\,, \quad u = (k-p')^2\,, \qquad (1)$$

with the constraint $s + t + u = 2M^2 + 2m^2$, where M and m are the masses of the nucleon and the electron, respectively. Furthermore, the four-momenta fulfill the on-shell conditions $k^2 = k'^2 = m^2$ and $p^2 = p'^2 = M^2$. In general the electrons can be considered to be massless, $m = 0$, because it requires highly relativistic energies to probe the internal structure of the nucleon. Finally, it is useful to introduce the crossing-symmetrical variable

$$\nu = \frac{s-u}{4M}\,, \qquad (2)$$

and to consider ν and t as the independent kinematical variables to describe the scattering process.

Due to the spins of the involved particles, we can define $2^4 = 16$ helicity amplitudes $T_{\alpha'\beta';\,\alpha\beta}$, where α and β are the helicities of the electrons and protons, respectively. If we neglect the electroweak currents, parity conservation yields the relation

$$T_{\alpha'\beta';\,\alpha\beta} = \text{phase} \cdot \mathrm{T}_{-\alpha'-\beta';\,-\alpha-\beta} \qquad (3)$$

which reduces the number of independent amplitudes to 8. A further reduction follows from time reversal invariance,

$$T_{\alpha'\beta';\,\alpha\beta} = \text{phase} \cdot \mathrm{T}^*_{\alpha\beta\,;\,\alpha'\beta'}\,. \qquad (4)$$

In conclusion we find 6 independent invariant amplitudes to describe electron-nucleon scattering, 3 of them conserving the helicity of the electron. Assuming parity and time-reversal invariance, the scattering matrix takes the form

$$T = \sum_{i=1}^{6} A_i(\nu,t)\,T_i\,, \qquad (5)$$

where the A_i are complex functions of the kinematical Lorentz invariants ν and t, and the T_i denote six independent combinations of the helicities, e.g., $(++ \to ++)$, $(++ \to +-)$, $(-+ \to -+)$ conserving the electron helicity and $(++ \to -+)$, $(++ \to --)$, $(-+ \to ++)$ changing the electron helicity. The latter 3 amplitudes vanish if the electron mass can be neglected.

The Mandelstam plane for electron-nucleon scattering is shown in Fig. 1 for highly relativistic electrons ($m = 0$). The physical region for the reaction $e + N \to e' + N'$ is given by the horizontally hatched area denoted "s channel". It is limited by the axis $t = 0$ (0° scattering) and a hyperbolically shaped curve at negative t values (180° scattering). The u-channel region to the left is related to the s-channel region by the symmetry under the crossing operation $\nu \to -\nu$. Finally, the physical reaction $e^+ + e^- \to N + \bar{N}$ occurs in the kinematical region, denoted by "t channel", which has its threshold at $t = 4M^2 \approx 3.5$ GeV^2. The dashed lines in Fig. 1 describe the onset of reactions that compete with elastic scattering. The lowest thresholds for such inelastic processes are given by pion electroproduction of a nucleon for $s = (M + m_\pi)^2$ and $u = (M + m_\pi)^2$ and electron-positron pair annihilation with the production of a two-pion system for $t = 4m_\pi^2$. Inside the triangle formed by the dashed lines, neither of these inelastic reactions can occur, and as a consequence the scattering amplitudes $A_i(\nu, t)$ are real functions in this area near the origin of the Mandelstam plane. Outside the triangle, we obtain the imaginary parts of the amplitudes by "cutting" the respective Feynman graphs and putting the intermediate particles on the mass shell. This is familiar for the process $e^- + e^+ \to \pi^- + \pi^+ \to N + \bar{N}$. Due to the existence of competing inelastic channels like $\pi^+\pi^-$, the scattering amplitudes (essentially the form factors) are complex functions for $t > 4m_\pi^2$. Since elastic electron scattering has usually been analyzed in the framework of the Born approximation, the scattering amplitudes in the s-

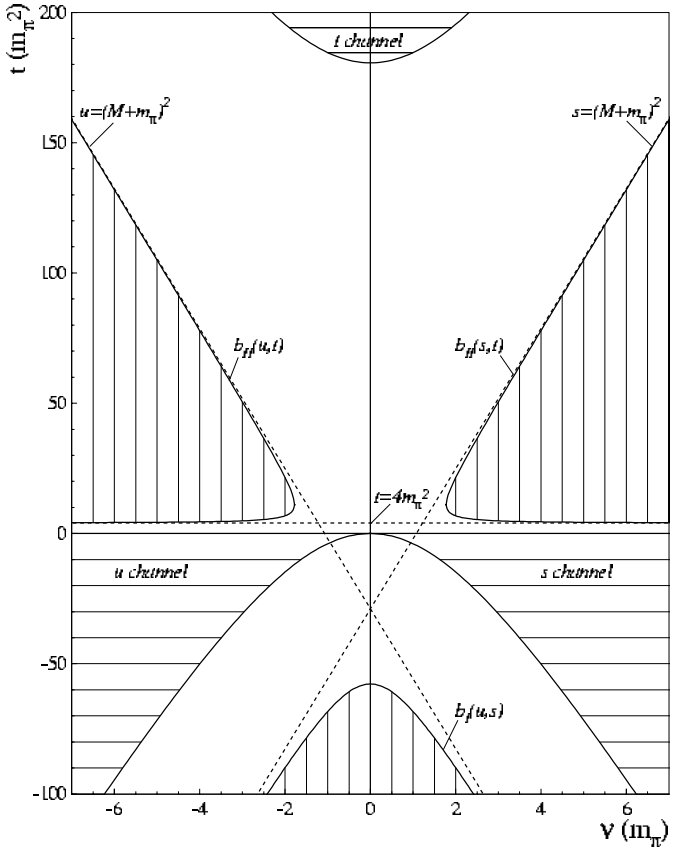

Fig. 1. The Mandelstam plane for highly relativistic electron-nucleon scattering. See text for explanation

and u-channel regions have been taken to be real. However, the exchange of 2 photons leads to an intermediate state for the reaction $e+N \to \tilde{e}+\tilde{N}+\pi \to e'+N'$, which results in an imaginary part of the scattering amplitude.

Though the two-photon physics is suppressed by the fine-structure constant $\alpha_{\rm em} \approx 1/137$, it may play an important role under kinematical conditions in which the Born approximation is small or vanishes. As an example, the Born approximation for electron scattering off a heavy nucleus, e.g. ^{208}Pb, leads to a series of zeros in the cross section, which are filled in by two-photon effects. These are, however, dominated by contributions with the intermediate nucleus being in its ground state, because in this case the photon couples to the total charge Z at each vertex. Contributions of single particle excitations are therefore suppressed by the huge factor of $1/Z^2$, and even collective excitations will involve only a fraction of the nucleons. The problem can therefore be solved by a partial wave analysis, which accounts for the deformation of the electron orbits by the static Coulomb potential but treats the nucleus as a rigid object. Experimental and theoretical investigations of so-called dispersion effects, contributions of intermediate excited states to electron scattering, were never quantitatively successful for several computational reasons, the coupling to a large number of bound states and a complicated continuum of break-up reactions, and one principal reason, namely that such an analysis requires a full-fledged analysis of inelastic scattering before hand. In view of these complications, electron scattering off light nuclei and in particular off the proton, has usually been treated in the Born approximation. Some exceptions of this are the early work on the dispersion corrections for the proton [1], and the search for the magnetic monopole transition [2]. However, we are now seeing a revival of the two-photon physics [3] because of two observations that have been made possible by recent precision experiments:

- The ratio G_E^p/G_M^p as function of Q^2 turns out to be constant if the differential cross section is analyzed by the Rosenbluth plot. The same ratio drops nearly linear and tends to a zero at $Q^2 \approx 8$ GeV^2 if evaluated from recent polarization data at the JLab [4].
- The electric proton r.m.s radius r_E^p as determined by electron scattering is about 0.84 fm [12], whereas atomic physicists derived values around 0.90 fm [5].

We conclude this section with a brief review on the invariant amplitudes in elastic electron-nucleon scattering. Assuming parity and time reversal invariance, there are 6 complex amplitudes A_i depending on 2 kinematical variables, e.g., ν and t. If we further neglect the mass of the highly relativistic electron, only 3 amplitudes contribute to the scattering process. In the Born approximation one more variable vanishes and all the information is contained in 2 form factors, say the electric (G_E^N) and magnetic (G_M^N) Sachs form factors. Because there is no dispersion in ν, these form factors only depend on one variable, namely $t = q^2 = -Q^2$. As a result, the current operator for space-like photons ($Q^2 > 0$) can be expressed by two real form factors. In particular in the Breit frame, the current takes the simple form

$$J_N^\mu = (\rho_N, \mathbf{j}_N) = \left(G_E^N\ (Q^2)\,,\ \frac{i\boldsymbol{\sigma} \times \mathbf{q}}{2m}\, G_M^N\ (Q^2) \right) . \quad (6)$$

2 Dispersion relations

The virtual photon as produced by pair annihilation is time-like, and therefore we can discuss the process in the photon's c.m. frame. The quantum numbers of the photon are $\mathcal{J}^{PC} = 1^{--}$, i.e., spin 1 and odd under both parity and charge conjugation. The isospin is not fixed, it can be $I = 0$ or 1. The imaginary part of the scattering amplitude originates from the fact that the photon can decay into any hadronic intermediate state before the final-state $N\bar{N}$ pair is produced, provided that the above quantum numbers are conserved. The lightest intermediate states consists of two pions. The required value $\mathcal{J} = 1$ corresponds to a relative P state, which is odd under particle exchange. In order to have overall Bose symmetry, the state vector has to be odd in isospace, too, which is only possible for $I = 1$. Therefore the isovector photon couples only to two-pion states with $I^G(\mathcal{J}^{PC}) = 1^+(1^{--})$, with a positive G parity as for any even number of pions involved. The first important resonance in that channel is the $\rho(770)$. The lightest intermediate states coupling to the isoscalar photon are the three-pion systems with quantum number

$0^-(1^{--})$, which also include the resonances $\omega(783)$ and $\phi(1020)$.

The form factor in the space-like region ($t = -Q^2 < 0$) is a real function which can be constructed as the Hilbert transform of the imaginary part of the amplitude or, in short, the spectral function. A generic form of such a dispersion relation takes the form

$$G^{V,S}(Q^2) = \frac{1}{\pi} \int_{t_{thr}}^{\infty} \frac{\mathrm{Im\,G^{V,S}(t')}}{t' + Q^2}\, dt' \,, \quad Q^2 \geq 0 \qquad (7)$$

where $t_{thr} = 4m_\pi^2$ for the isovector (V) and $t_{thr} = 9m_\pi^2$ for the isoscalar (S) channel. The spectral function for the isovector form factor has been constructed from other available data via the relation [6]

$$\mathrm{Im\,G^V(t)} = \mathrm{factor} \cdot \mathrm{F_\pi^*(t)\, T_{\pi\pi\to N\bar{N}}} \,, \qquad (8)$$

where $F_\pi(t)$ is the pion form factor describing the production of the two-pion system and $T_{\pi\pi\to N\bar{N}}$ is the scattering matrix that connects the two pions with quantum numbers $\mathcal{J}^{PC} = 1^{--}$ to an $N\bar{N}$ state carrying the same quantum numbers and isospin $I = 1$. The pion form factor is very well known, but $T_{\pi\pi\to N\bar{N}}$ has to be constructed in an unphysical region. This can be achieved by an analytic continuation of the respective pion-nucleon scattering matrix, which in practice works in the region $t_{thr} \leq t \lesssim 1$ GeV^2. Beyond this value, $\mathrm{Im}\, G^V$ is usually modelled by higher vector mesons. Unfortunately, the isoscalar part has to be modelled by vector mesons over the full t range. Being based on pion-nucleon scattering data, (8) contains all the correlations within the two-pion state and all the rescattering processes leading to the final $N\bar{N}$ state. In particular F_π and $T_{\pi\pi\to N\bar{N}}$ are complex functions, both carrying exactly the phase of the respective pion-pion system, $\delta(I = 1, \mathcal{J} = 1)$, as long as the t-channel energy is below the four-pion threshold.

A schematic picture of the magnetic proton form factor as function of t shows the following features: In the region $t = -Q^2 < 0$ (electron scattering), this form factor decreases with increasing values of Q^2 essentially like a dipole form, and for large Q^2 it approaches the Q^{-4} behavior required by asymptotic QCD. The range $4m_\pi^2 \leq t \leq 4M^2$ describes the unphysical region, which is dominated by (virtual) production of many-pion systems. In particular, the strong coupling of the photon to several vector mesons produces large fluctuations of the form factor, which clearly shows the importance of the spectral region. The form factors in the unphysical region have recently been constructed from the available space-like and time-like data by means of dispersion relations [7]. The physics of the storage rings starts at $4M^2$. Due to the existence of the spectral region to the right of the origin ($t = 0$), the measured time-like form factors for $t > 4M^2$ are larger than the space-like form factors at the same $|t|$ by about a factor of 3 to 4. It is therefore obvious that t values of at least 10 GeV^2 will be necessary to reach the realm of asymptotic QCD, which requires that the form factors take exactly the same value for space-like and time-like photons at sufficiently large values of $|t|$.

3 Chiral perturbation theory

As has been mentioned before, the spectral region of the form factors starts with two-pion intermediate states, which yield the tail of the density distribution at large distances. It is therefore interesting to study the model-independent predictions of ChPT for the spectral function. As an example, the spectral function of the isovector electric Sachs from factor takes the form

$$\begin{aligned} \mathrm{Im}\, G_E^V = \tfrac{1}{64\pi f_\pi^2 \sqrt{t}} \Big\{ \tfrac{2}{3} k_t \, \left[g_A^2 \,(5t - 8m_\pi) + 4k_t^2 \right] \\ - \tfrac{g_A^2}{M} \left(1 - 2m_\pi^2\right)^2 \left(1 + \tfrac{3t}{8M^2}\right) \arctan\left(\tfrac{2k_t\sqrt{4M^2 - t}}{t - 2m_\pi^2}\right) \\ + \tfrac{g_A^2\, k_t}{M^2} \left(t - 2m_\pi^2\right) \Big\} \,, \end{aligned} \qquad (9)$$

where $k_t = \sqrt{t/4 - m_\pi^2}$ is the pion momentum in the c.m. system, $g_A \approx 1.26$ the axial coupling constant, and $f_\pi \approx 93$ MeV the pion decay constant. Equation (9) represents the result at the one-loop order. The two-loop terms and the respective low-energy constants are given in [8], which also contains an excellent introduction to the field. The punch line is that (9) should not be further expanded as a power series in $1/M$, as usually done in HBChPT, because such an expansion destroys the proper analytic structure of the spectral function. In particular, it is straightforward to obtain the correct k_t^3 behavior of the P-wave pions from the unexpanded form. Below threshold, for $t < 4m_\pi^2$, k_t becomes imaginary. As a consequence the expression that describes the imaginary part in (9) now contributes to the real part of the form factor. Furthermore it is easy to work out that the argument of the arctan becomes i at $t = t_c = 4m_\pi^2 - m_\pi^4/M^2 \approx 3.98 m_\pi^2$. As can be seen from the relation $\arctan(x) = \int^x dx'/(1 + x'^2)$, the arctan has a singularity if the upper limit of the integral approaches $\pm i$. Though this singularity is not on the physical plane, its appearance so close to threshold leads to a dramatic enhancement of the two-pion component in the spectral function.

The predictions of the full two-loop order are shown for the two Sachs form factors by the full lines in Fig. 2. The comparison with the results of dispersion relations (dotted lines) shows the importance of the $\rho(770)$, which however can be added to ChPT with a reasonable choice of strength and width of that resonance (dashed lines). Unfortunately, it is not possible to extend the dispersion analysis to values much above $t = 40m_\pi^2$. Seeing that both ChPT and DR predict a positive definite spectral function in the region $t \lesssim 40m_\pi^2$, we conclude that there must be a considerable strength with negative sign above that region in order to yield an overall dipole shape of the form factors. Unfortunately there is not enough information about the heavier vector mesons in order to really predict the spectral function in the region $40m_\pi^2 \lesssim t \lesssim 4M^2$. The masses and coupling strengths of some of these heavier vector mesons are therefore taken as fit parameters in order to obtain a realistic description of the form factors within the dispersion analysis. Turned into the language of ChPT, it also takes LEC's beyond the physics of the $\rho(770)$ to describe form factors of the dipole form.

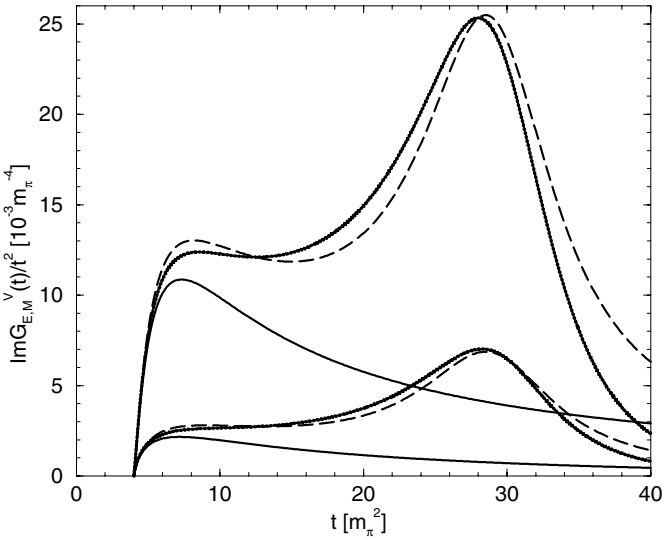

Fig. 2. Spectral functions of the isovector electric (*lower 3 lines*) and magnetic (*upper 3 lines*) Sachs form factors weighted with $1/t^2$. *Dotted lines:* dispersion relation [6], *full lines:* ChPT [8], *dashed lines:* ChPT plus ρ-meson contribution. Figure from [8]

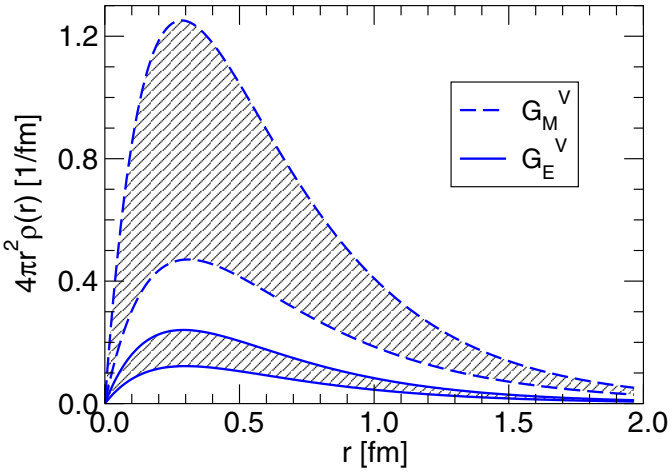

Fig. 3. The densities of charge and magnetization due to the pion cloud, $4\pi r^2\rho(r)$ for the electric (*lower band*) and isovector magnetic (*upper band*) Sachs form factors [9]

4 The role of the pion cloud

In view of the presented results of ChPT and DR, it is legitimate to ask, how much contributes the pion cloud to the spatial extension of the charge distribution? In order to answer this question we have to Fourier transform the Sachs form factors as defined in the Breit or brickwall frame, $q = (0, \mathbf{q})$. As an example we obtain

$$G_E(\mathbf{q}^2) = \int d^3r \rho_E(\mathbf{r}) e^{i\mathbf{q}\cdot\mathbf{r}} = e_N - \tfrac{1}{6}\,\mathbf{q}^2\langle r^2\rangle_E^N + \ldots \quad (10)$$

$$\rho_E(\mathbf{r}) = \frac{1}{(2\pi)^3}\int d^3q\, G_E(\mathbf{q}^2)\, e^{-i\mathbf{q}\cdot\mathbf{r}}\,. \quad (11)$$

Of course, this procedure is meaningful only for small space-like momentum transfers, within a region $\tau = Q^2/4M^2 = -t/4M^2 < 1$. The parameter τ measures the relativity, in particular $\tau = -1$ defines the onset of nucleon pair production. In the complex t-plane we have to stay well inside the circle $|\tau| < 1$, if we want to use non relativistic notions of single particle wave functions and spatial structure. Beyond this circle relativistic effects like boosts and Lorentz contractions will inevitably dominate the behavior of the form factors.

With this caveat in mind, let us try to answer the question raised above. For simplicity of notation we first define the spectral function for a form factor, $\sigma_i(\mu^2) = \mathrm{Im}\, G_i(\mu^2)$. Next we Fourier transform (7) according to (11) and obtain the generic form

$$\rho_i(r) = \frac{1}{4\pi^2}\int_{\mu_{thr}}^{\infty} d\mu^2\, \sigma_i(\mu^2)\,\frac{e^{-\mu r}}{r}\,, \quad (12)$$

a superposition of Yukawa terms with increasing mass μ. Since the spectral function does not seem to have a zero crossing in the low-mass region, we can at once give an upper limit for the r.m.s. radius,

$$\langle r^2\rangle_i \le \frac{6}{\mu_{thr}^2}\,, \quad (13)$$

with an upper limit obtained if all the strength is concentrated at threshold. Numerically this corresponds to radii $r^V < 1.72$ fm and $r^S < 1.15$ fm for the isovector and isoscalar form factors, respectively. The question about the pion contribution can, of course, only be answered qualitatively, because the extraction of the two-pion term from the full spectral function is somewhat model-dependent. Guided by ChPT and quite realistic models of the $\rho(770)$, we obtain the results presented in Fig. 3 for the distributions of charge and magnetization due to the "pion cloud" [9]. The seemingly large difference between charge and magnetization is essentially due to the usual normalization, $G_E^V(0) = (e_p - e_n)/2 = 0.5$, $G_M^V = (\mu_p - \mu_n)/2 = 2.353$. Integrated over all distances, the pion cloud contributes about 30 % to the total charge of the proton and 30 % to $\langle r^2\rangle_E^V$. The pion contribution normalized to itself has $\langle r^2\rangle^\pi \approx 1$ fm^2, substantially outside of the proton radius $\langle r^2\rangle_E^p \approx 0.74$ fm^2. Since the pion contribution is smoothly distributed over a relatively large region, its Fourier components will die out much faster with increasing Q^2 than the contributions of heavier mass systems (vector mesons, quark core). Therefore, the overall dipole factor with mass $\mu_{dip} = 0.84$ GeV can not be expected to describe the form factors over the full Q^2 range. The evidence for a pionic component in the form factors is clearly seen, such as in a recent comparison of the world data with a phenomenological pion-cloud plus quark-core model [10]. Our analysis agrees with these findings qualitatively, although we find a considerably smaller pionic density at radii above 1 fm and a correspondingly smaller radius of the pionic distribution.

5 Lattice calculations

While all other theories and models have their shortcomings in terms of adjustable parameters, lattice calculations hold the promise to yield absolute predictions based on QCD. Unfortunately, the lattice calculations still have to go a long way to yield quantitative results even for relatively simple observables like form factors. At present the main drawback of such calculations is the large quark mass that has to be used for numerical reasons. As an example, Fig. 4 shows the results of [11] for the isovector Pauli radius calculated with "pion masses" between 500 MeV and 1 GeV. Expressed in terms of the threshold for the spectral function, this corresponds to $t_{thr} \gtrsim 50\, m_\pi^2$ instead of the physical value $4m_\pi^2$. As a result the (physical) pion cloud effects will be essentially wiped out, and indeed the lattice results predicts a much too compact structure of $\langle r^2\rangle_2^V \approx 0.4$ fm^2, while the dispersion analysis of the data yields a value of about 0.8 fm^2. In this situation it is a very promising strategy to combine ChPT and lattice calculations. While the former can not predict the anomalous magnetic moments or the radii themselves, it allows solid predictions about how these observables depend on the pion mass. As we can see from Fig. 4, the rapid increase of the radius does not become visible until the pion mass has been reduced to about 200 MeV, and therefore the long-range tail of the density distribution can not be described by present lattice gauge calculations. The role of the pion cloud stands out most clearly in the case of the electric form factor of the neutron, which is essentially described by a negative pion cloud around a positively charged quark core. As a result a recent lattice calculation of [13] with $m_\pi \gtrsim 500$ MeV found only a tiny neutron radius corresponding to about 20% of the experimental value of $\langle r^2\rangle_E^n = -0.116$ fm^2. However, in lack of any other parameter-free theory within sight, our only hope remains a gradual numerical and analytical progress in lattice calculations in order to connect the nucleon's properties directly with QCD.

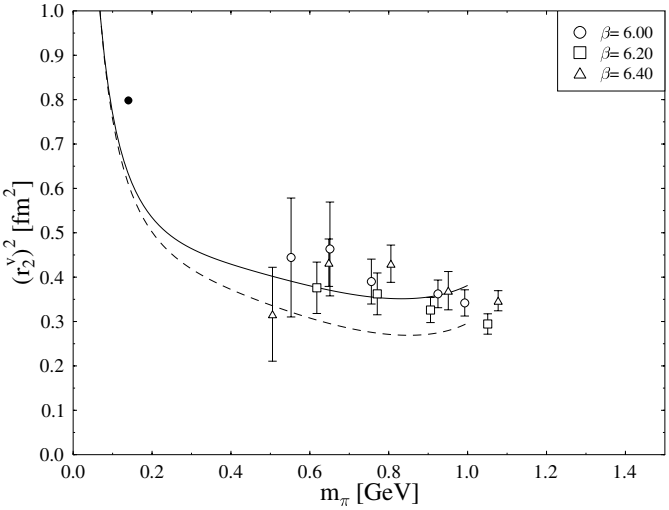

Fig. 4. The isovector Pauli radius obtained from lattice calculations [11] as function of the pion mass (*open symbols*). The *full circle* is the result of dispersion relations [12]. The *full* and *dashed lines* are chiral extrapolations to smaller pion masses, see [11] for details

6 Transition form factors

The form factors of a transition from the nucleon N to a resonance R can be formally defined in a covariant way,

$$G_m = \langle R,\, \lambda' = m - \tfrac{1}{2} \mid \epsilon_m^\mu \cdot J_\mu \mid N,\, \lambda = -\tfrac{1}{2}\rangle\,, \quad (14)$$

where λ and λ' are the helicities of the nucleon and of the resonance, respectively. The index m denotes the helicity transferred by the electromagnetic field, which is characterized by 2 transverse polarization vectors $\epsilon_{(\pm)}^\mu = \frac{1}{\sqrt{2}}\,(0, \mp, -i, 0)$, a longitudinal polarization vector $\epsilon_{(0)}^\mu = \frac{1}{Q^2}\,(q, 0, 0, \omega)$, and a virtual photon with four-momentum $q^\mu = (\omega, 0, 0, q)$. Equation (14) yields 3 independent form factors for each resonance, the 3 transitions starting from $\lambda = +\frac{1}{2}$ follow from parity conservation.

The form factors of (14) are related to the more familiar helicity amplitudes [17],

$$A_{1/2} = \sqrt{\tfrac{2\pi\alpha}{k_\gamma}}\,\langle R,\, \tfrac{1}{2} \mid \tfrac{J_x + iJ_y}{\sqrt{2}} \mid N,\, -\tfrac{1}{2}\rangle\, \xi \sim G_+\,,$$
$$A_{3/2} = \sqrt{\tfrac{2\pi\alpha}{k_\gamma}}\,\langle R,\, \tfrac{3}{2} \mid \tfrac{J_x + iJ_y}{\sqrt{2}} \mid N,\, \tfrac{1}{2}\rangle\, \xi \sim G_-\,,$$
$$S_{1/2} = -\sqrt{\tfrac{2\pi\alpha}{k_\gamma}}\,\langle R,\, \tfrac{1}{2} \mid \rho \mid N,\, \tfrac{1}{2}\rangle\, \xi \sim G_0\,,$$

where use has been made of the continuity equation $\omega\rho = q\, J_0$. The additional factor ξ is the phase of the decay matrix element $R \to N\pi$. It has been introduced to make the helicity amplitudes independent of arbitrary overall phases of the wave functions. If the resonance has a spin $J \geq \frac{3}{2}$, both $A_{3/2}$ and $A_{1/2}$ contribute and appropriate linear combinations of them are defined as electric (G_E) and magnetic (G_M) form factors. The charge matrix element for resonance excitation is then usually dubbed G_C, which is somewhat confusing, because in the case of elastic scattering it is traditionally called G_E.

We also note that the concept of resonance form factors is based on the notion of a zero width resonance. The actual observables are, e.g., electric ($E_{\ell\pm}$), magnetic ($M_{\ell\pm}$), and charge ($S_{\ell\pm}$) multipoles that are complex functions of momentum transfer (Q^2) and total c.m. energy (W). Therefore, the derivation of real form factors $G_i(Q^2)$ requires some analysis which is by no means model independent.

For an isolated resonance like the $\Delta(1232)$ we may use a Breit-Wigner ansatz that factorizes the multipole into the product of a (real) reduced multipole, say $\bar{E}_{\ell\pm}(Q^2)$, and a Breit-Wigner form including some kinematical and resonance properties depending on W. This ansatz is then fitted to the data, and the reduced multipole follows from the imaginary part of the actual multipole at the reso-

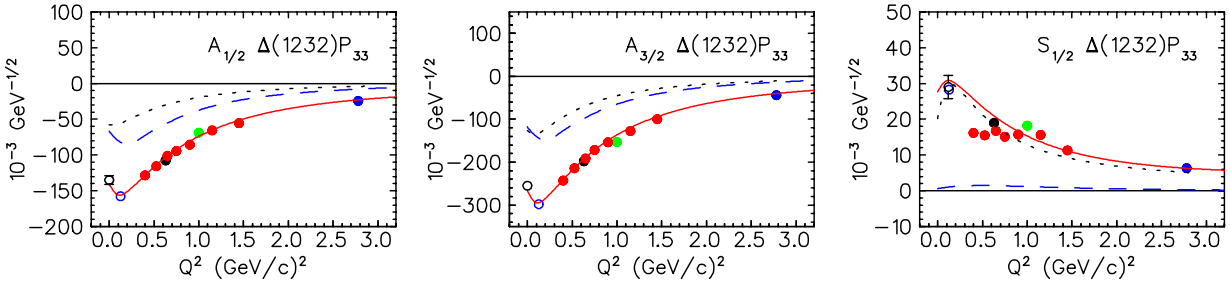

Fig. 5. The Q^2 dependence of the $N \to \Delta$ helicity amplitudes. The *solid* and *dashed curves* are the results of the superglobal fit with MAID [14] and the predictions of the hyperspherical constituent quark model [15]. The *dotted lines* show the pion cloud contributions calculated with the Dubna-Mainz-Taipei model [16]. See [17] for further details

nance position. It is quite obvious that this procedure will be even more model dependent in the case of overlapping resonances at the higher excitation energies.

As an example, the helicity form factors for the excitation of the $\Delta(1232)$ may be obtained as

$$\begin{aligned} A^{\Delta}_{1/2}(Q^2) &= -\tfrac{1}{2}\,(3\,\bar{E}_{1+}(Q^2) + \bar{M}_{1+}(Q^2))\,, \\ A^{\Delta}_{3/2}(Q^2) &= \tfrac{\sqrt{3}}{2}\,(\bar{E}_{1+}(Q^2) - \bar{M}_{1+}(Q^2))\,, \\ S^{\Delta}_{1/2}(Q^2) &= -\sqrt{2}\,\bar{S}_{1+}(Q^2)\,. \end{aligned} \qquad (15)$$

The simplest picture for the $N \to \Delta(1232)$ transition is a quark spin flip leading from the octet to the decuplet representation of SU(6). In concordance with this model, the transition is dominated by a magnetic dipole transition (M_{1+}), while the corresponding electric quadrupole transition (E_{1+}) is very small. On the other hand, asymptotic QCD requires that for sufficiently large Q^2 the amplitude $A_{3/2}$ should be suppressed relative to $A_{1/2}$, because the former transition can not take place on an individual quark with spin 1/2. Therefore, the ratio $R_{EM} = E_{1+}/M_{1+}$ should approach 1 for $Q^2 \to \infty$, while the existing data yield $R_{EM} \approx -2\%$ with a slight increase with growing Q^2 and some indication that R_{EM} crosses the zero line near $Q^2 = 4$ GeV^2. As a consequence of the small value of R_{EM}, (15) yields $A^{\Delta}_{3/2} \approx \sqrt{3}\,A^{\Delta}_{1/2}$, which is also obtained by all quark and many other models. However, if it comes to the absolute magnitude of these helicity amplitudes, the usual quark models underestimate the strength by 30% or more as is shown in Fig. 5 for the Genova hypercentral constituent quark model [15]. The failure to describe the data can again be traced to the missing pion cloud. Such effects can be studied more quantitatively in dynamical models like the Dubna-Mainz-Taipei model [16]. The essential point is that a pion can also be produced by a non-resonant mechanism (e.g., Kroll-Ruderman term), but then the pion rescatters from the nucleon, and because of unitarity the corresponding amplitude inevitably takes the phase δ_{1+} of the pion-nucleon system in the Δ region (Fermi-Watson theorem). In other words, the direct production of the Δ (say by a quark spin-flip) and the indirect production by means of rescattering add coherently in the physical amplitude. The contribution of the pion cloud is shown in Fig. 5 by the dotted lines, and by adding the quark model (dashed lines) and the pion cloud distributions, we obtain a nice agreement with the data. In the case of the charge transition $S_{1/2}$, the pion cloud is particularly important. This transition measures the induced charge quadrupole moment, which scales with r^2, the square of the distance to the nucleon's center. It is therefore no big surprise that the pion cloud at distances of 1 fm and beyond is much more effective than the quark core of typically 0.5 fm.

References

1. S.D. Drell, S. Fubini: Phys. Rev. **113**, 741 (1959); G.K. Greenhut: Phys. Rev. **184**, 1860 (1969)
2. N. Voegler et al.: Phys. Rev. C **43**, 2172 (1991); E. Borie, D. Drechsel: Phys. Lett. **26**, 195 (1971)
3. P. Blunden: these proceedings.
4. J. Arrington: Phys. Rev. C **68**, 034325 (2003); R. Segel: these proceedings
5. I. Sick: these proceedings
6. G. Höhler et al.: Nucl. Phys. B **114**, 505 (1976); H.-W. Hammer, U.-G. Meißner, D. Drechsel: Phys. Lett. B **385**, 343 (1996)
7. R. Baldini et al.: Eur. Phys. J. C **11**, 709 (1999)
8. N. Kaiser: Phys. Rev. C **68**, 025202 (2003)
9. H.-W. Hammer, D. Drechsel, U.-G. Meißner: Phys. Lett. B **586**, 291 (2004)
10. J. Friedrich, T. Walcher: Eur. Phys. J. A **17**, 607 (2003)
11. M. Göckeler et al.: hep-lat/0303019 (2003)
12. P. Mergell, U.-G. Meißner, D. Drechsel: Nucl. Phys. A **596**, 367 (1996)
13. A. Tang, W. Wilcox, R. Lewis: Phys. Rev. D **68**, 094503 (2003)
14. D. Drechsel, O. Hanstein, S.S. Kamalov, L. Tiator: Nucl. Phys. A **645**, 145 (1999); http://www.kph.uni-mainz.de/MAID/.
15. M.M. Giannini, E. Santopinto, and A. Vassallo, Eur. Phys. J. A **12** (2001) 447; Nucl. Phys. A **699** (2002) 308.
16. S. Kamalov, S.N. Yang, D. Drechsel, O. Hanstein, and L. Tiator, Phys. Rev. C **64** (2001) 032201; http://www.kph.uni-mainz.de/MAID/DMT/.
17. L. Tiator et al.: Eur. Phys. J. A **19**, 55 (2004)